Biophysical Journal, Volume *111*

Supplemental Information

Binding of Vinculin to Lipid Membranes in Its Inhibited and Activated States

Mridula Dwivedi and Roland Winter

Binding of Vinculin to Lipid Membranes in its Inhibited and Activated States

Mridula Dwivedi[†*] and Roland Winter[†*]

† Physical Chemistry I, Biophysical Chemistry, Faculty of Chemistry and Chemical Biology, TU Dortmund University, Otto-Hahn-Strasse 4a, D-44227 Dortmund, Germany

SUPPORTING INFORMATION

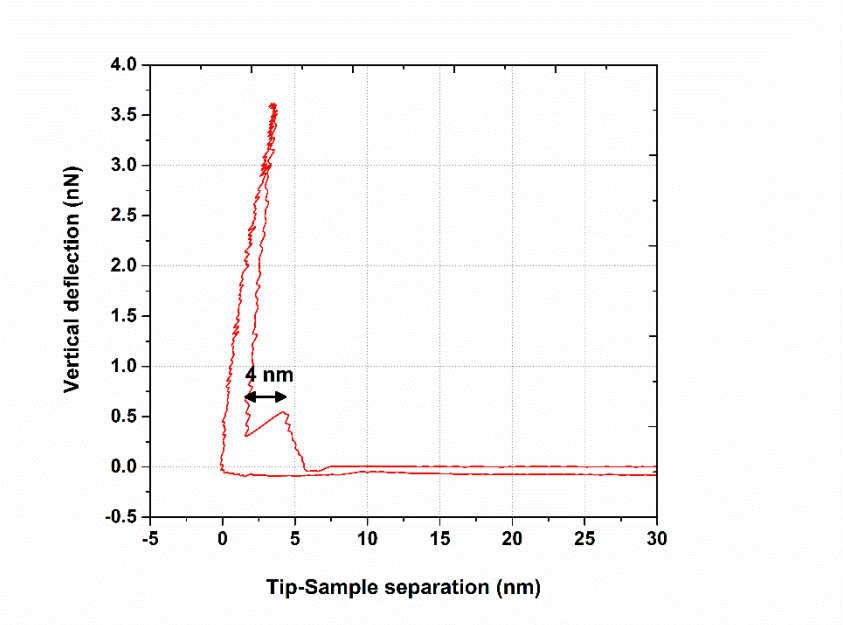

Figure S1. Force-distance curves measured on a homogenous membrane showing ~4 nm force-jumps, demonstrating the presence of a lipid bilayer.

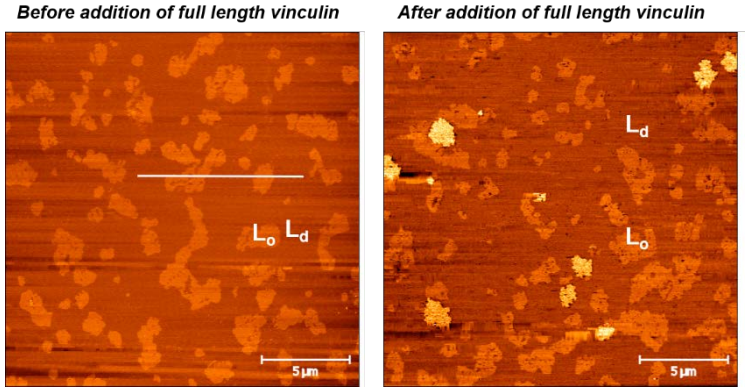

Figure S2. AFM images of a DPPC/DOPC/Chol (1:2:1) +0.8% PIP_2 lipid bilayer membrane on mica before and after injection of 40 nM full length vinculin. The absence of membrane defects and the liquid-ordered and liquid-disordered domains can be clearly observed and is marked. Addition of 40 nM vinculin causes preferential partitioning and clustering of the protein in the liquid-disordered phase.

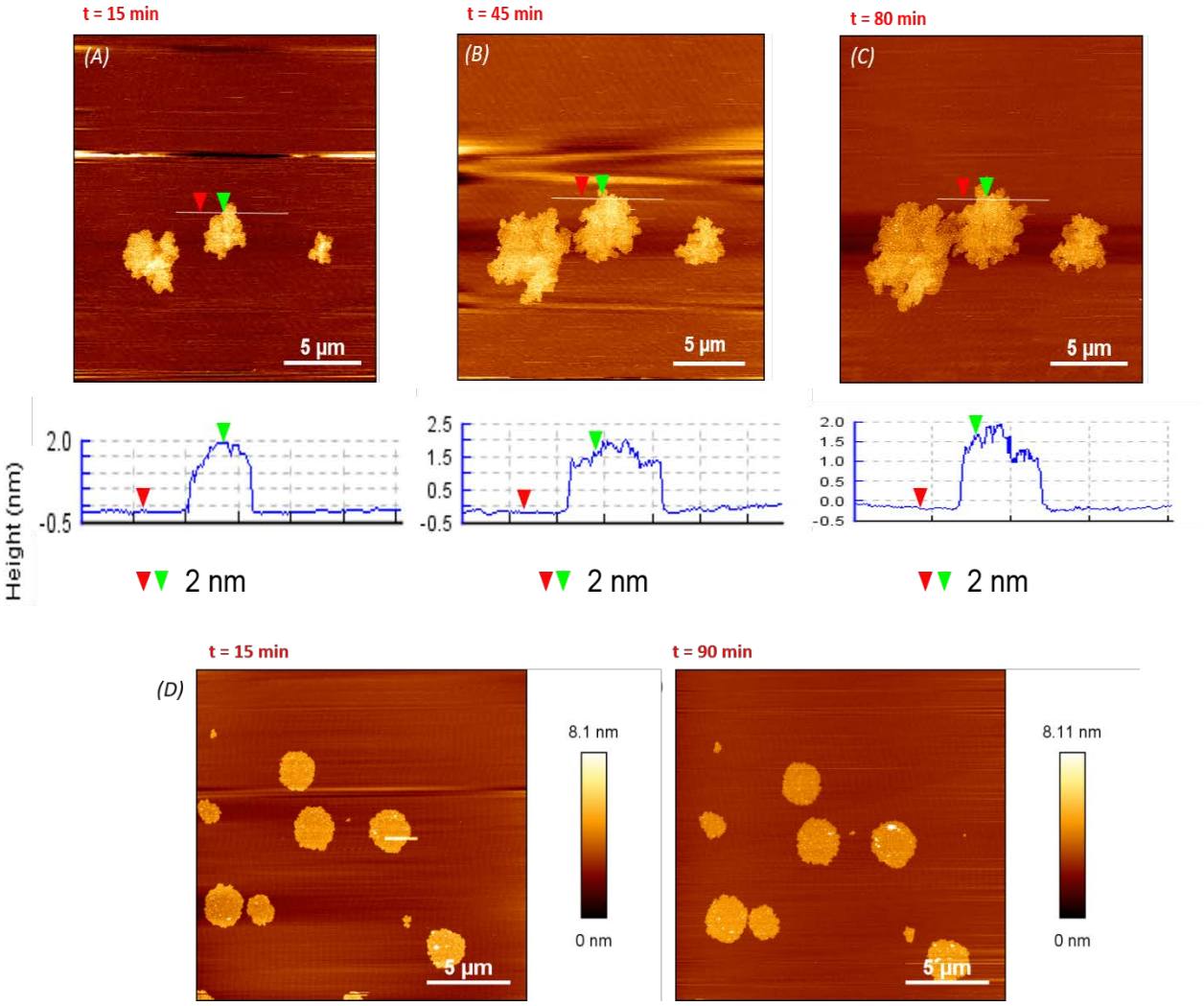

Figure S3. AFM images of a pure DOPC lipid membrane on mica after addition of 40 nM of vinculin solution in the presence of 150 mM NaCl (A), (B) and (C). The time series is represented from 15 mins from the addition of the protein solution to 80 min. The average cluster height is maintained in the range of 1.5 nm to 2 nm indicating lateral growth of clusters, only. (D) represents the corresponding AFM images at low ionic strength where the cluster size remains more or less constant over time.

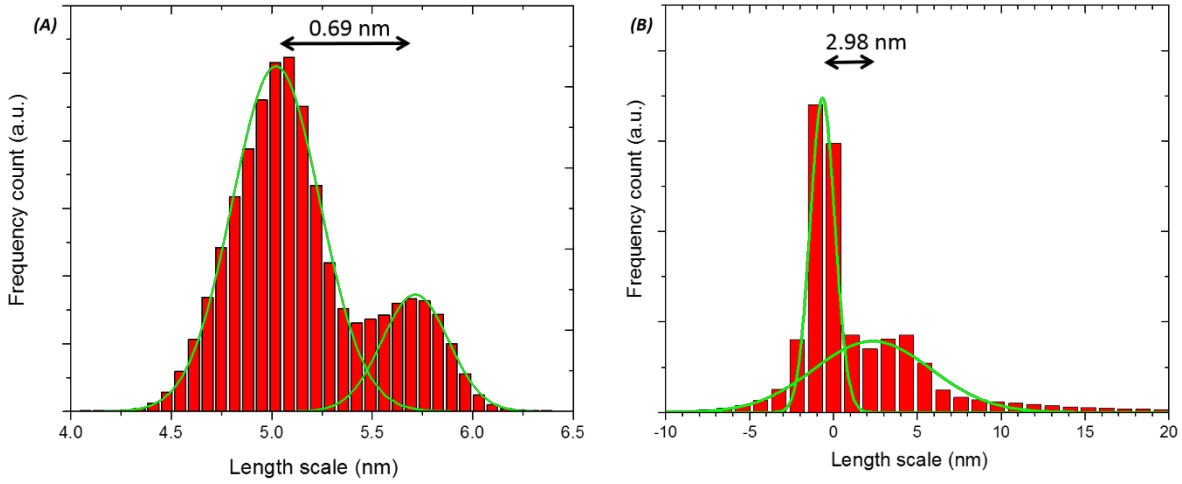

Figure S4. Histogram profile for (A) Figure 1A and (B) Figure 1B showing the height distribution over the image. The histogram height profile of Figure 1A shows the presence of phase separation with a height difference of 0.69 nm. The histogram profile of Figure 1B shows the difference between the bilayer and vinculin bound to the membrane with a height difference of 2.98 nm.

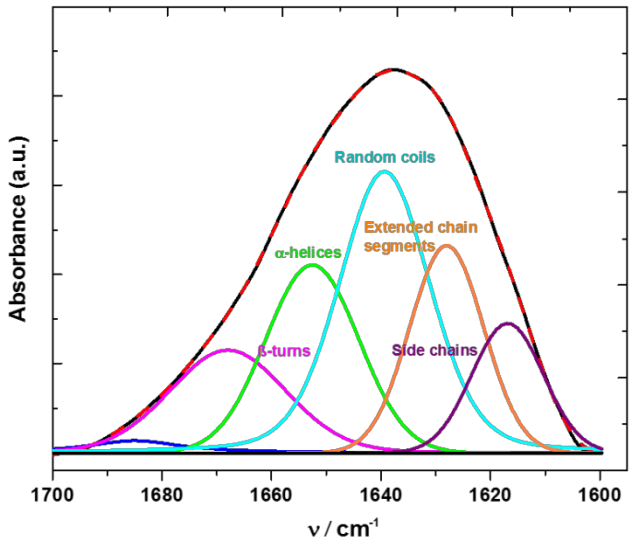

Figure S5. Conformational changes in vinculin monitored by FTIR spectroscopy. The figure shows normalized FTIR spectra of vinculin in bulk solution under denaturing temperature conditions (70 °C). The local minima and maxima from the second derivative and FSD, respectively, was used to detect the amide-I' sub-bands. The peak assignment was done taking into consideration the known X-ray data and the percent secondary structure was determined by calculating the area under the sub-peaks. The black curve herein represents the original spectrum and the red curve is the fitted curve.

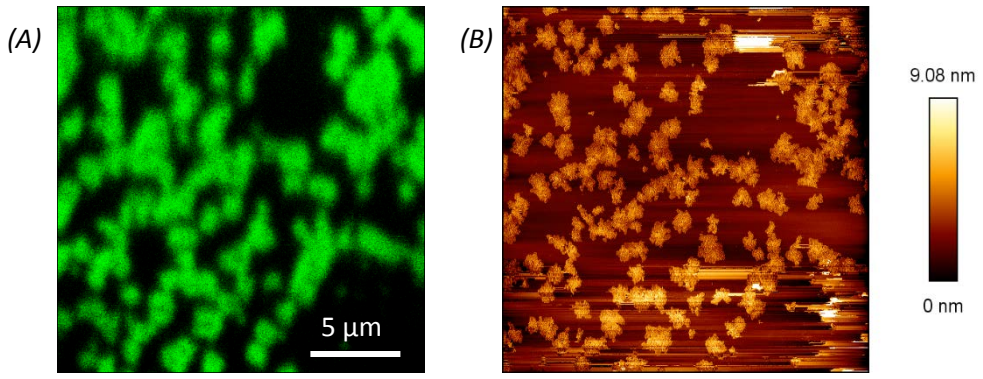

Figure S6. Fluorescence microscopy image *(A)* coupled with the corresponding atomic force microscopy image *(B)* of Cys-labelled unactivated vinculin adsorbed on a DOPC supported lipid bilayer.

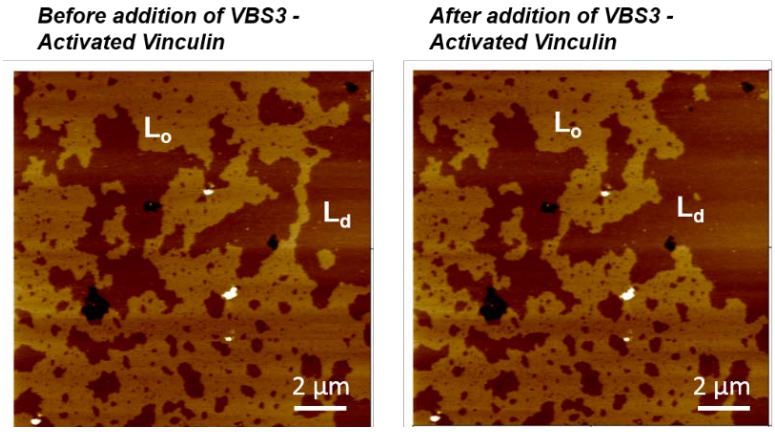

Figure S7. Atomic force microscopy images of a supported lipid bilayer with the lipid composition DPPC/DOPC/DPPG/DOPG/Chol (45:20:5:5:25) showing phase separation marked with L_o (liquid-ordered) and L_d (liquid-disordered). The addition of VBS3 activated vinculin did not show any noticeable binding to the supported lipid bilayer containing 10% negatively charged lipids, hence reinforcing the specificity of the VBS3 activated vinculin to PIP_2.

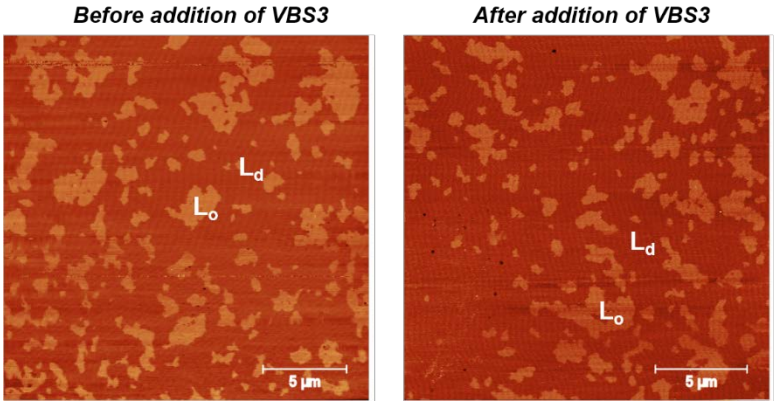

Figure S8. Atomic force microscopy images of a supported lipid bilayer with the lipid composition DPPC/DOPC/Chol (1:2:1) + 0.8% PIP_2 showing phase separation marked with L_o and L_d. Upon VBS3 addition, no significant binding is observed to the lipid bilayer.